Nanoscale

Accepted Manuscript

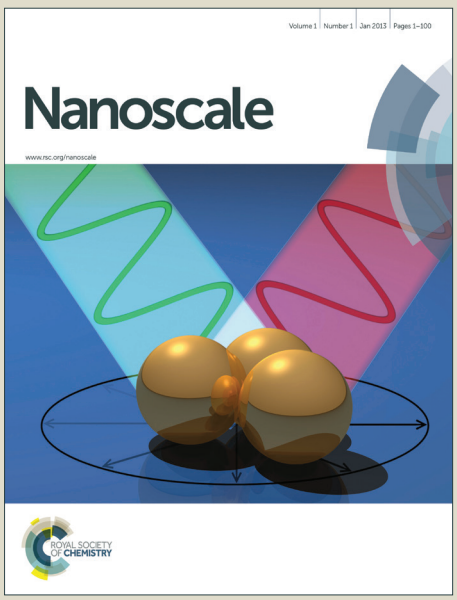

ROYAL SOCIETY OF CHEMISTRY

www.rsc.org/nanoscale

Nanoscale

RSCPublishing

ARTICLE

Silver Nanowire-embedded PDMS with Multiscale Structure for Highly Sensitive and Robust Flexible Pressure Sensor†

Cite this: DOI: 10.1039/xoxxoooooox

Received ooth January 2012,
Accepted ooth January 2012

DOI: 10.1039/xoxxoooooox

www.rsc.org/

Yunsik Joo [a], Junghwan Byun [a], Narkhyeon Seong [a], Jewook Ha [a], Hyunjong Kim [a], Sangwoo Kim [a], Taehoon Kim [a], Hwarim Im[a], Donghyun Kim[a] and Yongtaek Hong*[a]

Development of highly sensitive pressure sensor with a low-cost and facile fabrication technique is desirable for electronic skins and wearable sensing devices. Here a low-cost and facile fabrication strategy to obtain multiscale-structured elastomeric electrodes and a highly sensitive and robust flexible pressure sensor is presented. The principles of spontaneous buckle formation of PDMS surface and the embedding of silver nanowires are used to fabricate the multiscale-structured elastomeric electrode. By laminating the multiscale-structured elastomeric electrode onto the dielectric layer/bottom electrode template, the pressure sensor can be obtained. The pressure sensor is based on the capacitive sensing mechanism and shows high sensitivity (>3.8 kPa^{-1}), fast response and relaxation time (<150 ms), high bending stability and high cycle stability. The fabrication process can be easily scaled up to produce pressure sensor arrays and they can detect the spatial distribution of the applied pressure. It is also demonstrated that the fingertip pressure sensing device can sense the pressure distribution of each finger, when grabbing an object.

1. Introduction

Flexible, bendable or stretchable pressure sensors have gained exponential interest recently, because of their versatile application to the human oriented future technologies such as electronic skins,[1-4] wearable healthcare monitors,[5-8] prosthetic skins,[2,9,10] patient rehabilitation,[11,12] robotic skins[13-15] and touch interfaces.[16,17] For the realization of most of the aforementioned technologies that mimic human skin or human tactile receptors, highly sensitive pressure sensors for low pressure-regime (<10 kPa, gentle touch)[18] with mechanical flexibility or strecthability are required. Various sensing mechanisms have demonstrated the possibility to fabricate highly sensitive and flexible pressure sensors. They includes piezoresistive sensing,[5,19-24] piezoelectric sensing,[25-27] triboelectric sensing[27,28] and capacitive sensing mechanisms.[9,16,30-34] The piezoresistive sensors based on pressure sensitive rubber (PSR) have been widely investigated by being integrated with organic field effect transistors[1,4,15] or inorganic semiconducting nanowire-based transistors[3] for large area artificial electronic skins. Recently, a PSR based pressure sensor array fabricated with semiconducting carbon nanotube transistors and organic light-emitting diodes[35] and a piezoelectric nanowire light-emitting diode-based pressure sensor array[27] demonstrate the real-time visualization of pressure mapping. However, vacuum processes are needed for these sensor arrays and PSR based sensors are susceptible to hysteresis and show low stability.[13,36]

Capacitive pressure sensors with elastomeric dielectric materials also have been widely investigated.[17,30,32,34] The elastomeric dielectric layer is deformed (e.g., the thickness of the dielectric layer is reduced) when an external pressure is applied to the sensor and this deformation induces the capacitance change of the sensor. Various metals (gold, silver) or liquid metal have been used as electrodes of the capacitive pressure sensor.[17,34] Nanomaterials such as silver nanowires (AgNWs) or carbon nanotubes which have been widely investigated for stretchable electronics were also used with elastomeric dielectric layers for stretchable capacitive pressure sensors.[16,30,32,37] Although these sensors have mechanical stretchability, their pressure sensitivity is low. To enhance the pressure sensitivity of capacitive-type sensors, recently, microstructured elastomeric dielectric layers have been introduced and the pressure sensors with them show high pressure sensitivity and mechanical flexibility.[9,31] By integrating organic field effect transistors with the microstructured elastomer as a gate insulator, pressure sensitive active sensor devices have been fabricated.[9,31] However, the manufacturing process of the mould for microstructured

elastomers is based on the photolithography and chemical etching, which are expensive and complicated processes.

In this work, we present a highly sensitive and flexible capacitive pressure sensor with the multiscale-structured elastomeric electrode by using a simple and low-cost process. The spontaneous buckle formation of ultraviolet/ozone (UV/O_3) treated pre-strained PDMS[38] was used as a simple and low cost mould fabrication method. Through this mould, the AgNWs embedded multiscale-structured PDMS electrode was fabricated. By sandwiching the multiscale-structured electrode and a solution processed dielectric layer/electrode template, the flexible capacitive pressure sensor can be obtained. The sensor shows high sensitivity (3.8 kPa^{-1}), fast response and relaxation time (< 150 ms), high flexibility and high stability. In addition, the pixel-type pressure sensor array can be easily fabricated and scaled up from the simple cutting and attaching process. The fingertip grip pressure sensing device is also demonstrated by attaching each sensor onto the fingertips.

2. Results and Discussion

The multiscale-structured PDMS electrode was fabricated as schematically illustrated in Fig. 1a. To obtain the multiscale-structured electrode, we used the spontaneous buckle formation of PDMS surface due to the relaxation of pre-stretched PDMS with stiff silicon oxide film[38] as a mould. Initially, the mould PDMS was stretched up to 40%, and then treated with ultraviolet/ozone (UV/O_3) radiation to introduce silicon oxide (SiO_X) thin film on the surface of PDMS. After that, AgNW solution was coated onto the mould PDMS by using a bar coater for several times to obtain resistance below 30 Ω for electrodes with 40 mm length and 30 mm width. After obtaining the AgNW film, the mould PDMS was released to its initial length (zero strain) to obtain the buckled AgNW film. Due to the preformed silicon oxide thin film on the mould PDMS surface, the buckled structure was introduced on the PDMS surface[38] and the AgNW film also showed the buckled surface as shown in Fig. 1b. The liquid PDMS with curing agent was poured on the buckled AgNW film, and then cured at 65 °C for 12 h in air. Due to the penetration of the liquid PDMS into the AgNW network, the AgNW film was embedded tightly into the cured PDMS.[38] By peeling off the mould PDMS, we obtained the AgNW-embedded multiscale-structured PDMS as shown in Fig. 1b. The AgNW-embedded surface of PDMS is conductive and the opposite surface of PDMS is non-conductive. The resistances of the AgNW film (20Ω) and the multiscale-structured electrode (45Ω) at each fabrication stage are indicated in Fig. 1b. The resistance of the AgNW film was increased slightly after strain releasing (25Ω) due to the rearrangement of each AgNW and AgNW junctions. The resistance of the AgNW-embedded multiscale-structured PDMS electrode was increased over 100% after peeling off due to the penetration and filling of the AgNW junctions of PDMS and the peel-off stress.[39,40]

The capacitive pressure sensor was fabricated by integrating the multiscale-structured electrode with dielectric layer and bottom electrode (Fig. 1c). The bottom Ag electrode was inkjet-printed on the flexible Arylite substrate and the dielectric layer was spin-coated onto the bottom electrode (Fig. 1c). Poly(methyl methacrylate) (PMMA) or poly(4-vinylphenol) (PVP) was used as a dielectric layer (We will call the dielectric layer coated bottom electrode as the bottom plane). The detailed printing or spin coating method was described in our previous works[41,42] and the experimental section. Copper wire was connected to the multiscale-structured electrode by silver paste for electrical measurement. Finally, the multiscale-structured electrode was laminated onto the dielectric layer with the multiscale structure facing the dielectric layer to fabricate the capacitive pressure sensor.

The multiscale structure of the AgNW-embedded PDMS electrode was characterized by using scanning electron microscopy (SEM), 3-D surface profiler and atomic force microscopy (AFM). The multiscale structure consists of the wavy structure (micrometer-size) obtained from the buckled PDMS mould and the rough surface of the crest of the wavy structure (nanometer-size) obtained from the relaxation of peel-off stress, as shown in Fig. 2 and Fig. S1 in ESI†. The uniform wavy structure of the AgNW-embedded PDMS was characterized by using SEM. The average wavelength and amplitude of the wavy structure are about 22 μm and 6 μm, respectively, as shown in Fig. 2a and 2b. Fig. 2a and 2b also show that the wavy structure was formed uniformly over the entire region and AgNWs were totally embedded into the PDMS matrix. The rough surface of the crest was observed from 3-D surface profiler and AFM images (see Fig. 2c and 2d). When peeling off the cured PDMS, the peel-off stress was applied to the entire domain of the AgNW-embedded PDMS. More excessive peel-off stress was applied to the sharp crest of the wavy structure among the entire domain and the rough surface was formed spontaneously to release the peel-off stress at the crest (The surface of the trough of the wavy structure is much smoother than the crest and this means that the smaller peel-off stress is applied to the trough, as shown in Fig. S1c, ESI†).[39, 40] However, no rough surface of the crest was observed from the structured PDMS without AgNWs as shown in Fig. 2e and 2f. The root-mean-square (RMS) values of the measured line roughness at the crest are about 350 nm for AgNW-embedded PDMS and 30 nm for only PDMS, respectively. The AgNW-embedded PDMS is still flexible, bendable and deformable as reported elsewhere.[16,30,39] The resistance of the wavy structured electrode was hardly changed from its original value during the repeated pressing (up to 10 kPa) (see ESI, Fig. S2†).

Pressure was applied to the capacitive pressure sensor to test the pressure sensitivity. The force gauge with z-axis motor stage and weights were used as pressure applying tools. The size of the square pressure sensitive capacitor was 16 mm^2 (the size of the multiscale-structured electrode is 4 × 10 mm^2). To avoid the stickiness of PDMS that could hinder the pressure sensor test, the poly(ethylene terephthalate) (PET) film (100 μm) was attached on the PDMS surface and thin glass slide was placed onto the PET film. The pressure from the multiscale-structured electrode with PET film and glass slide (180 mg) is defined as the base pressure (45 Pa) and the capacitance at the base pressure is defined as the base capacitance $\boldsymbol{C_0}$. The external pressure was applied from 0 Pa to 4.5 kPa. Fig. 3a shows the pressure sensitivities of the sensors with the multiscale-structured electrode and non-structured flat electrode, respectively. The pressure sensitivity of the pressure sensor ($\boldsymbol{S}$) can be defined as the slope of the relative capacitance change-pressure curve in Fig. 3a ($\boldsymbol{S} = \boldsymbol{\delta(\Delta C/C_0)/\delta p}, \boldsymbol{\Delta C = C - C_0}$, where $\boldsymbol{C}$ and $\boldsymbol{C_0}$ denote the capacitance with the applied pressure and the base capacitance, respectively, and $\boldsymbol{p}$ denotes the applied pressure). The sensor with non-structured electrode (flat electrode in Fig. 3a) shows no change of capacitance according to the applied pressure.

However, the sensor with the multiscale-structured electrode shows high sensitivity of 3.8 kPa^{-1} in the low pressure regime (45 ~ 500 Pa), 0.8 kPa^{-1} in the mid pressure regime (500 Pa ~ 2.5 kPa) and 0.35 kPa^{-1} in the high pressure regime (2.5 ~ 4.5 kPa). The sensitivity of our sensor surpassed that of the previously reported capacitive pressure sensors for a wide pressure regime (0 ~ 4.5 kPa).[9,31] The pressure sensor with the multiscale-structured electrode shows very small hysteresis (see ESI, Fig. S3†). The pressure sensor can detect the loading and unloading of a paper ship of very small weight (40 mg) as shown in Fig. 3b. The pressure of the paper ship is about 15 Pa. The capacitance change of the sensor is large enough to detect the small pressure. Ten independent sensors were measured to check the sample-to-sample variation in pressure sensitivity and the average capacitance values at each pressure are plotted with error bars (standard deviation) as shown in Fig. S4, ESI†. Pressure sensors fabricated by using multiscale-structured electrodes obtained from the mould PDMS with different pre-strain level were also tested to check the variation of pressure sensitivity according to the pre-strain level of the mould PDMS, as shown in Fig. S5, ESI†. The variation of pressure sensitivity was small. Therefore, we used the mould PDMS with pre-strain level of 40% only based on this result.

This dramatic high pressure sensitivity of the pressure sensor can be based on the multiscale structure (it consists of the wavy structure and the rough surface of the crest) and the deformable property of the electrode. The AgNW-embedded PDMS electrode can be deformed by the applied pressure or external force. From this property, the contact area and the volume of air gap between the multiscale-structured electrode and dielectric layer are changed by the applied pressure. Therefore, when the pressure is applied to the sensor, the sharp contact edges of the wavy structure and the rough surface of the crest provide dramatic changes of the contact area and the volume of air gap. Through these changes of the contact area and the volume of air gap, the capacitance of the sensor changes dramatically and the sensor shows high pressure sensitivity. Due to the rubberlike property of the multiscale-structured electrode, any kind of the dielectric layer that shows higher mechanical rigidity than the multiscale-structured electrode can be used to the sensor. Polymer dielectric materials such as PMMA and PVP can be applied to the sensor as a dielectric layer as shown in Fig. 3a. Even oxide dielectric material can be used to the sensor. (see ESI, Fig. S6†). Each sensitivity of the sensors was similar, with the variation below 10 %, regardless of the kind of polymer dielectric layer.

Fig. 3c and insets show the response and relaxation times of the sensor. When the pressure of 1.5 kPa was loaded and unloaded to the sensor, the response and relaxation times were less than 150 ms, respectively. When the pressure like stair shape, a rising and falling pressure (400 Pa → 1500 Pa → 400 Pa → no load), is applied, the response and relaxation times are less than 500 ms and the capacitance shows the same value for the same pressure regardless of the previous pressure (Fig. 3d). The capacitance of the sensor does not change for the static pressure, which means the stable operation of the sensor for the static pressure and demonstrates the accurate measurement for the applied pressure (Fig. 3c and d).

The stability of the pressure sensor was investigated from the repeated loading/unloading cycling test. The capacitance changes of the sensor were measured when the pressure of 1.5 kPa was loaded and unloaded repeatedly up to 1500 times as shown in Fig. 4a. The capacitance of the sensor at each pressure was hardly changed for repeated cycles. The result indicates that the pressure sensor has high stability for the repeated loading/unloading. In addition, the bending stability of the sensor was tested by using a home-made bending apparatus. For the bending test, the multiscale-structured electrode was fastened to the bottom plane by using a Kapton tape. The relative capacitance change- pressure curve of the sensor were measured before bending and after 5000-cycle bending with 3 mm radius of curvature. The relative capacitance changes of the 5000-cycle bending tested sensor at each pressure show no appreciable degradation in comparison with the as-prepared sensor (Fig. 4b). The pressure sensor with the multiscale-structured electrode is robust and stable to the repeated loading/unloading and bending cycles based on the above results.

The AgNW-embedded multiscale-structured PDMS electrode can be easily handled and scaled up for a large-area fabrication. Simply, by cutting and attaching the multiscale-structured PDMS electrode of desired size onto the PET substrate (50 μm thick), we fabricated pixel-type capacitive pressure sensor arrays. The bottom Ag electrode was inkjet-printed and PVP dielectric layer was spin-coated. As shown in Fig. 5a and 5d, sensor arrays with 3 × 3 pixels and 5 × 5 pixels were obtained (size of the sensor array is 24 × 24 mm^2) and the sizes of each capacitor were 4 × 4 mm^2 and 2 × 2 mm^2, respectively. To investigate the sensing ability of the sensor arrays, a small weight (5 g, 8 mm diameter) was loaded to the marked site of the sensor array with 3 × 3 pixels as shown in Fig. 5a and 5b. The corresponding result is visualized to a two-dimensional intensity profile as shown in Fig. 5c. It is notable that the loaded site only shows a large increment of capacitance and other sites show small increments of capacitances. Also, the large increment value that obtained from this array device is similar to that of the single sensor device for 1.5 kPa pressure. We also fabricated the sensor array with 5 × 5 pixels that has much smaller size of pixel (2 × 2 mm^2). This 5 × 5 sensor array has a smaller sensing area per pixel than 3 × 3 array (Fig. 5d). Small weights (1 g, 6 mm diameter and 2g, 6mm diameter) were loaded onto the marked sites as shown in Fig. 5d and 5e. The corresponding result is visualized to a two-dimensional intensity profile as shown in Fig. 5f. The capacitances of the sites with weights only increase dramatically. The increment value of the site with 2g weight is higher than those of the sites with 1g weight and the increment values of the sites with 1g weight are almost same. These results from sensor arrays of 3 × 3 pixels and 5 × 5 pixels demonstrate that the sensor arrays can detect the spatial distribution of the applied pressure with the sensitivity as high as that of the single sensor and be applied to the electronic skins or large area wearable sensing devices.

Our pressure sensor can be used to measure the pressures of fingertips when an object is grabbed with fingers. To realize the fingertip pressure sensing prototype device, each sensor was attached on the four fingers except a little finger as shown in Fig. 6a. The capacitor size of each finger sensor was 4 × 4 mm^2 and PMMA was used as a dielectric layer. The plastic beaker (28.11 g) was grabbed tightly not to drop it down by the four fingers (Fig. 6b). Fig. 6c shows each capacitance change ratio ($\Delta C/C_0$) of the pressure sensors attached on the four fingers. The capacitance change ratio of the sensor on the thumb is about 7.6, the largest value among the fingertip sensors, which means that the highest pressure was applied to the thumb among the four fingers when the beaker was grabbed. The capacitance change ratio of the index finger is the second largest (5), that of the middle finger is third (4.6) and that of the ring finger is forth (3.2). The result demonstrates that the

pressure sensor can be used to sense the fingertip pressure distribution, when grabbing an object. Our pressure sensor can be applied to the finger or hand muscles rehabilitation treatment to measure the degree of the grip strength of the patient and the sportswear to measure the distribution of pressures or forces of people's hands when grabbing a ball, a bat, a racket, a golf club, etc.

3. Conclusions

In summary, we developed capacitive pressure sensors based on the robust and elastomeric AgNW-embedded multiscale-structured PDMS electrode with a low-cost and simple fabrication process for the first time. The capacitive pressure sensor has high pressure sensitivity 3.8 kPa^{-1} (45 ~ 500Pa), 0.8 kPa^{-1} (500 Pa ~ 2.5 kPa) and 0.35 kPa^{-1} (2.5 ~ 4.5 kPa) and can detect very small pressure of 15 Pa. The sensor also shows fast response and relaxation times (< 150 ms), high stability for repeated cycles over 1500 times and high bending stability. We demonstrated easy handling and scaling up of our sensor by fabricating 3 × 3 and 5 × 5 arrays. These arrays also show high pressure sensitivity similar to the single sensor device and can detect the spatial distribution of the applied pressure. We also fabricated the fingertip pressure sensing device to detect the pressure distribution of fingers, when grabbing an object. The highly sensitive and stable capacitive pressure sensor with a low-cost fabrication and easy handling may open and broaden its application to wearable electronic skins for rehabilitation treatment of patients and pressure mapping in sports activities or daily activities.

4. Experimental

4.1. Preparation of the multiscale-structured electrode

The mould PDMS was prepared by mixing the liquid PDMS elastomer (Sylgard 184, Dow corning) and a curing agent in the ratio 10:1 by weight. The liquid mixture was poured onto a glass substrate and thermally cured at 130 °C for 20 min. The cured PDMS was cut into rectangles (8 cm × 10 cm) and placed onto the glass substrate. After that, we stretched the PDMS uniaxially up to 40% with tweezers, and fixed the both ends of PDMS with binder clips. The stretched PDMS was UV/O_3-treated (power = 28 mW cm^{-2}) for 30 minutes to form the SiO_X thin film on the PDMS surface. AgNWs (SLV-NW-90, Blue Nano inc.) were tip-sonicated (52 W, 10 minutes) to obtain the length of 5 ~ 10 μm. AgNWs were bar-coated onto the stretched and UV/O_3 treated PDMS several times through the Arylite mask (3 cm × 4 cm) to obtain the resistance below 30 Ω. The bar-coated AgNW film was dried at 60 °C for 30 min. After the heat treatment, AgNW coated PDMS was released to its original condition (no strain) to introduce the spontaneous buckle formation. Finally, the liquid mixture of a liquid PDMS elastomer and a curing agent (10:1, w/w) was casted onto the buckled surface of the AgNW coated PDMS, followed by curing at 65 °C for 12 h. After the curing process, we inverted the cured PDMS/mould PDMS and then peeled off the mould PDMS from the AgNW-embedded PDMS while the AgNW-embedded PDMS is attached to the glass by using tweezers.

4.2. Fabrication of Pressure sensors and arrays

The Ag ink (Sigma-Aldrich) was printed on the flexible Arylite substrate (200 μm thickness, Ferrania Corp.) by using a piezoelectric inkjet-printer (DMP-2831, Dimatix Corp.), and then sintered at 100 °C for 1 h. A PMMA solution containing 10 wt% of PMMA (M_w ~120,000, Sigma-Aldrich) dissolved in propylene glycol methyl ether acetate (PGMEA) or a PVP solution containing 10 wt% of PVP (M_w ~30,000, Sigma-Aldrich) and 2 wt% of poly(melamine-co-formaldehyde) as a cross-linking agent dissolved in PGMEA was spin-coated on the Ag printed Arylite substrate for the formation of the dielectric layer. Afterward, the PMMA film was dried at 120 °C for 1h and the PVP film was cross-linked at 200 °C for 1 h. The pressure sensors were fabricated by laminating the multiscale-structured electrode (A pressure of 10 kPa was applied to the multiscale-structured electrode before the lamination) on top of the dielectric layer/Ag printed Arylite substrate and thin PET film (50, 100 μm thickness, Toray Corp.) was placed on top of the multiscale-structured PDMS to avoid the stickiness of PDMS during the pressure sensing tests. Both electrodes were connected to copper wire with silver paste for electrical measurements. For 3 × 3 and 5 × 5 sensor arrays, the multiscale-structured electrodes were cut into 2 mm × 22 mm and 4 mm × 22 mm respectively by a razor blade and attached to PET film to form pixel type arrays. For the fingertip pressure sensors, we stuck elastomeric foam-tape (3M™ VHB™ Tape) on the poly glove and laminated each bottom plane on the tape. After that, we sandwiched the multiscale-structured electrode on the bottom plane by using Kapton tape to fabricate the pressure sensors.

4.3. Microstructural characterization and measurements

The microstructure of the AgNW-embedded multiscale-structured PDMS electrode was characterized by a field emission scanning electron microscope (FE-SEM, Hitachi S-48000), a 3-D surface profiler (NanoFocus) and AFM (XE-100, Park Systems Corp.). For the 3-D surface profiler measurement, thin gold layer (20nm) was deposited on the PDMS and AgNW-embedded PDMS by using thermal evaporator. The microscopic images were obtained by an optical microscope (EGTECH). Capacitance was measured at 1 kHz with a 0.1 V a.c. signal by using the Agilent 4284A LCR meter. IMADA force gauge with z-axis stage was used to apply the pressure to the sensor and metal or plastic weights were used to apply the pressure to the arrays and the sensor. A mechanical bending test was performed using a home-made bending apparatus.

Acknowledgements

This work was supported by the Center for Advanced Soft-Electronics funded by the Ministry of Science, ICT and Future Planning as Global Frontier Project, Korea (Code No. 2012M3A6A5055728)

Notes and references

[a] Department of Electrical and Computer Engineering
Inter University Semiconductor Research Center (ISRC)
Seoul National University

Seoul, 151–742, Republic of Korea
E-mail: yongtaek@snu.ac.kr

†Electronic Supplementary Information (ESI) available. See DOI: 10.1039/b000000x/

1 T. Someya, T. Sekitani, S. Iba, Y. Kato, H. Kawaguchi and T. Sakurai, *Proc. Natl. Acad. Sci. USA,* 2004, **101**, 9966.
2 A. N. Sokolov, B. C.-K. Tee, C. J. Bettinger, J. B.-H. Tok and Z. Bao, *Acc. Chem. Res.,* 2012, **45**, 361.
3 K. Takei, T. Takahashi, J. C. Ho, H. Ko, A. G. Gillies, P. W. Leu, R. S. Fearing and A. Javey, *Nat. Mater.,* 2010, **9**, 821.
4 T. Sekitani and T. Someya, *MRS Bull.,* 2012, **37**, 236.
5 C. Pang, G.-Y. Lee, T.-I. Kim, S. M. Kim, H. N. Kim, S.-H. Ahn and K-Y. Suh, *Nat. Mater.,* 2012, **11**, 795.
6 X. Wang, Y. Gu, Z. Xiong, Z. Cui and T. Zhang, *Adv. Mater.,* 2014, **26**, 1336.
7 G. Schwartz, B. C.-K. Tee, J. Mei, A. L. Appleton, D. H. Kim, H. Wang and Z. Bao, *Nat. Commun.,* 2013, **4**, 1859.
8 W. Honda, S. Harada, T. Arie, S. Akita and K. Takei, *Adv. Funct. Mater.,* 2014, **24**, 3299.
9 S. C. B. Mannsfeld, B. C.-K. Tee, R. M. Stoltenberg, C. V. H.-H. Chen, S. Barman, B. V. O. Muir, A. N. Sokolov, C. Reese and Z. Bao, *Nat. Mater.,* 2010, **9**, 859.
10 E. Biddiss and T. Chau, *Med. Eng. Phys.,* 2006, **28**, 568.
11 L. Masia, H. I. Krebs, P. Cappa and N. Hogan, *IEEE/ASME Trans. Mechatronics*, 2007, **12**, 399.
12 M. Donati, N. Vitiello, S. M. M. D. Rossi, T. Lenzi, S. Crea, A. Persichetti, F. Giovacchini, B. Koopman, J. Podobnik, M. Munih and M. C. Carrozza, *Sensors*, 2013, **13**, 1021.
13 N. Lu and D.-H. Kim, *Soft Robotics*, 2013, **1**, 53.
14 H.-K. Lee, S.-I. Chang and E. Yoon, *J. Microelectromech. Syst.,* 2006, **15**, 1681.
15 T. Someya, Y. Kato, T. Sekitani, S. Iba, Y. Noguchi, Y. Murase, H. Kawaguchi and T. Sakurai, *Proc. Natl. Acad. Sci. USA,* 2005, **102**, 12321.
16 S. Yao and Y. Zhu, *Nanoscale*, 2014, **6**, 2345.
17 D. P. J. Cotton, I. M. Graz and S. P. Lacour, *IEEE Sens. J.,* 2009, **9**, 2008.
18 E. S. Dellon, R. Mourey and A. L. Dellon, *J. Plast. Reconstr. Surg.,* 1992, **90**, 112.
19 B. C.-K. Tee, C. Wang, R. Allen and Z. Bao, *Nat. Nanotechnol.,* 2012, **7**, 825.
20 H.-B. Yao, J. Ge, C.-F. Wang, X. Wang, W. Hu, Z.-J. Zheng, Y. Ni and S.-H. Yu, *Adv. Mater.,* 2013, **25**, 6692.
21 L. Pan, A. Chortos, G. Yu, Y. Wang, S. Isaacson, R. Allen, Y. Shi, R. Dauskardt and Z. Bao, *Nat. Commun.,* 2014, **5**, 3002.
22 B. Zhu , Z. Niu , H. Wang , W. R. Leow , H. Wang , Y. Li , L. Zheng, J. Wei, F. Huo and X. Chen, *Small*, 2014, **10**, 3625.
23 J. Lee , S. Kim, J. Lee, D. Yang, B. C. Park, S. Ryu and I. Park, *Nanoscale*, 2014, **6**, 11932.
24 Q, Shao, Z. Niu, M. Hirtz, L. Jiang, Y. Liu, Z. Wang and X. Chen, *Small,* 2014, **10**, 1466.
25 J. Chen, K. Y. Lee, C.-Y. Kang, M. W. Kim, S.-W. Kim and J. M. Baik, *Adv. Funct. Mater.,* 2014, **24**, 2038.
26 C. Hou, T. Huang, H. Wang, H. Yu, Q. Zhang and Y. Li, *Sci. Rep.,* 2013, **3**, 3138.
27 C. Pan, L. Dong, G. Zhu, S. Niu, R. Yu, Q. Yang, Y. Liu and Z. L. Wang, *Nat. Photonics*, 2013, **7**, 752.
28 F.-R. Fan, L. Lin, G. Zhu, W. Wu, R. Zhang and Z. L. Wang, *Nano Lett.*, 2012, **12**, 3109.
29 L. Lin, Y. Xie, S. Wang, W. Wu, S. Niu, X. Wen and Z. L. Wang, *ACS Nano*, 2013, **7**, 8266.
30 W. Hu, Z. Niu, R. Zhao and Q. Pei, *Appl. Phys. Lett.,* 2013, **102**, 083303.
31 J. Kim, T. N. Ng and W. S. Kim, *Appl. Phys. Lett.,* 2012, **101**, 103308.
32 D. J. Lipomi, M. Vosgueritchian, B. C.-K. Tee, S. L. Hellstrom, J. A. Lee, C. H. Fox and Z. Bao, *Nat. Nanotechnol.,* 2011, **6**, 788.
33 K. F. Lei, K.-F. Lee and M.-Y. Lee, *Microelectron. Eng.,* 2012, **99**, 1.
34 H. Vandeparre, D. Watson and S. P. Lacour, *Appl. Phys. Lett.,* 2013, **103**, 204103.
35 C. Wang, D. Hwang, Z. Yu, K. Takei, J. Park, T. Chen, B. Ma and A. Javey, *Nat. Mater.,* 2013, **12**, 899.
36 M. Hussain, Y.-H. Choa and K. Niihara, *J. Mater. Sci. Lett.,* 2001, **20**, 525.
37 Z. Niu, H. Dong, B. Zhu, J. Li, H. H. Hng, W. Zhou, X. Chen and S. Xie, *Adv. Mater.,* 2013, **25**, 1058.
38 C. Yu and H. Jiang, *Thin Solid Films*, 2010, **519**, 818.
39 F. Xu and Y. Zhu, *Adv. Mater.,* 2012, **24**, 5117.
40 C. H. Lee, D. R. Kim and X. Zheng, *Proc. Natl. Acad. Sci. USA*, 2010, **107**, 9950.
41 S. Chung, S. O. Kim, S.-K. Kwon, C. Lee and Y. Hong, *IEEE Electron Device Lett.,* 2011, **32**, 1134.
42 S. Chung, M. Jang, S.-B. Ji, H. Im, N. Seong, J. Ha, S.-K. K, Y.-H. Kim, H. Yang and Y. Hong, *Adv. Mater.,* 2013, **25**, 4772.

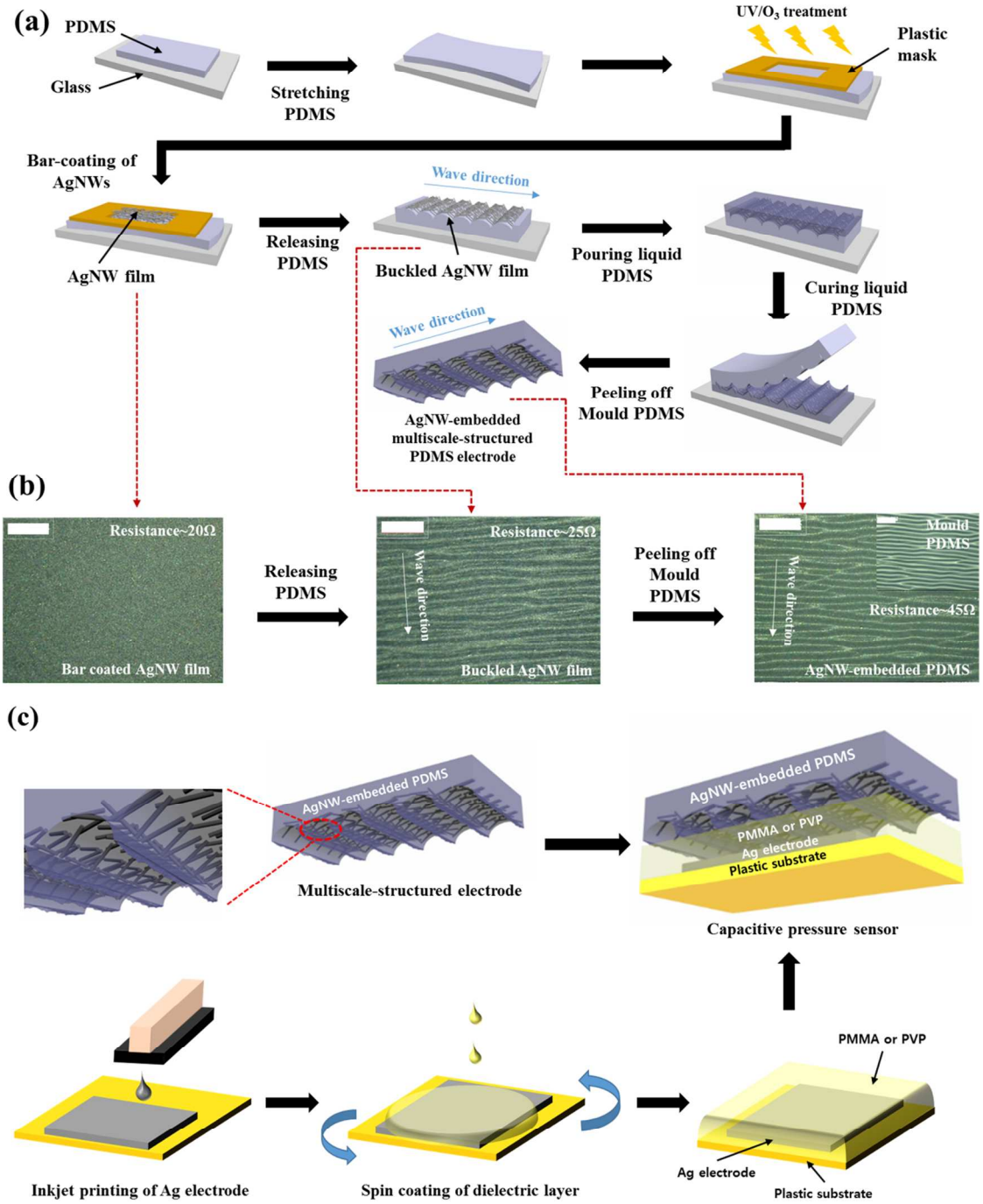

Fig. 1 Fabrication process of the multiscale-structured electrode and the capacitive pressure sensor. (a) Schematic diagrams of the fabrication process of the AgNW-embedded multiscale-structured PDMS electrode. (b) Microscopic images of the AgNW film at each fabrication step. AgNW film was bar-coated on the PDMS (left). Buckled AgNW film was formed after strain releasing (middle). The buckled AgNWs were totally embedded into the PDMS and AgNWs were hardly left on the mould PDMS (right). (Scale bar = 100 μm). (c) Schematic diagrams of the fabrication process of the capacitive pressure sensor. The capacitive pressure sensor is obtained by laminating the multiscale-structured electrode onto the bottom plane comprised of inkjet-printed Ag electrode and spin coated dielectricl layer.

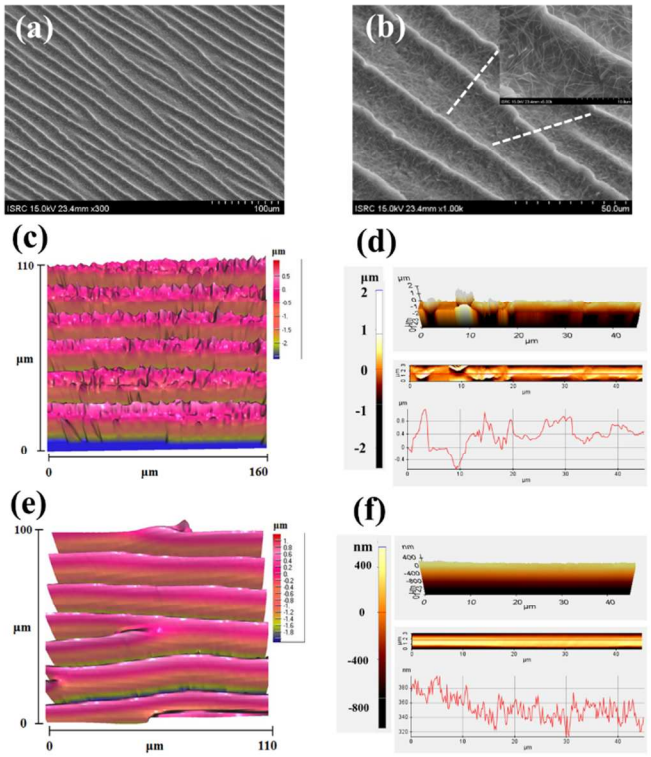

Fig. 2 The microstructure of the multiscale-structured electrode. (a) SEM image of the multiscale-structured electrode with high uniformity. (b) AgNWs are totally embedded into the PDMS and the high magnification inset image shows that AgNWs are embedded well even in the crest of the wavy structure. (c) 3-D surface profiler image of the multiscale-structured electrode. The rough surface at the crest of wavy structure is formed. (d) AFM image and line profile of the crest of the multiscale-structured electrode. In this crest, the root-mean-square (RMS) value of the measured line roughness is about 350 nm. (e) 3-D surface profiler image of the structured PDMS (AgNWs were not bar-coated onto the mould PDMS. It means that the bar-coating of AgNWs is omitted from the fabrication process in Fig. 1a). (f) AFM image and line profile of the crest of the structured PDMS. In this crest, the root-mean-square (RMS) value of the measured line roughness is about 30 nm.

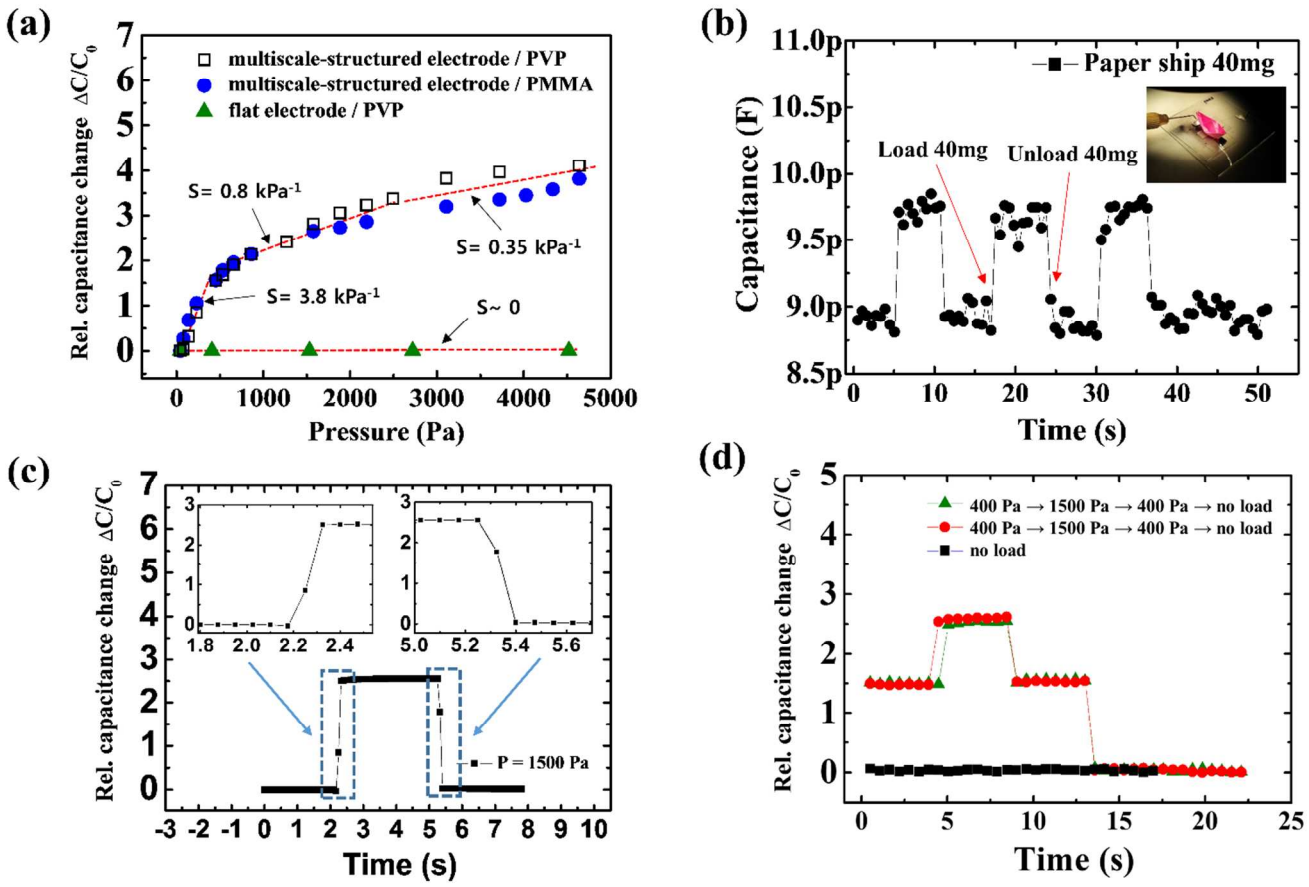

Fig. 3 Characterization of the capacitive pressure response of the pressure sensor. (a) Relative capacitance change-pressure curve for the multiscale-structured electrode with PVP or PMMA dielectric layer and the non-structured flat electrode with PVP dielectric layer. The sensors with the multiscale-structured electrode exhibit higher pressure sensitivity than the sensor with non-structured electrode. (b) Capacitance-time curve for the detection of very small pressure (15 Pa) according to the loading and unloading of a paper ship (40mg). (c) Fast response and relaxation time (< 150 ms) of the sensor. (d) Stair-like pressure loading and unloading. The sensors show fast response and relaxation regardless of the previous pressure.

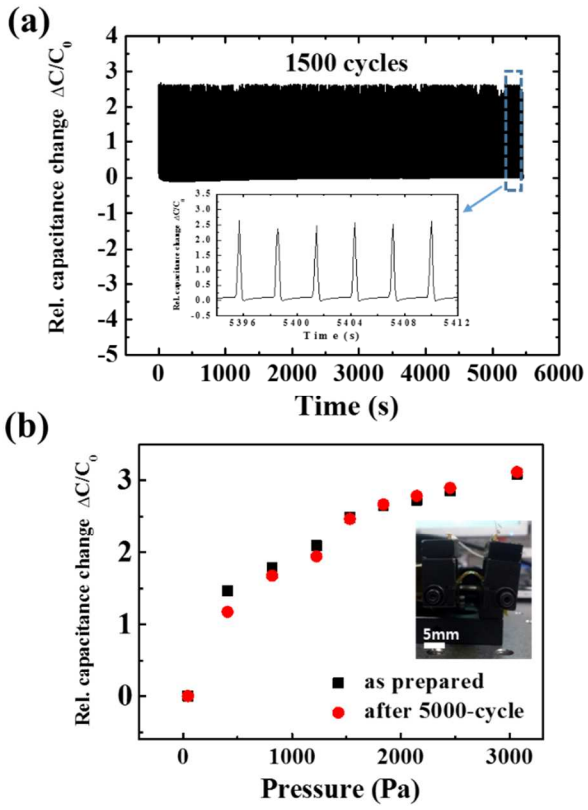

Fig. 4 Stability of the pressure sensor. (a) Stability of pressure response to the 1500-cycle loading/unloading pressure of 1500 Pa. (b) Bending stability of pressure response after 5000-cycle bending test.

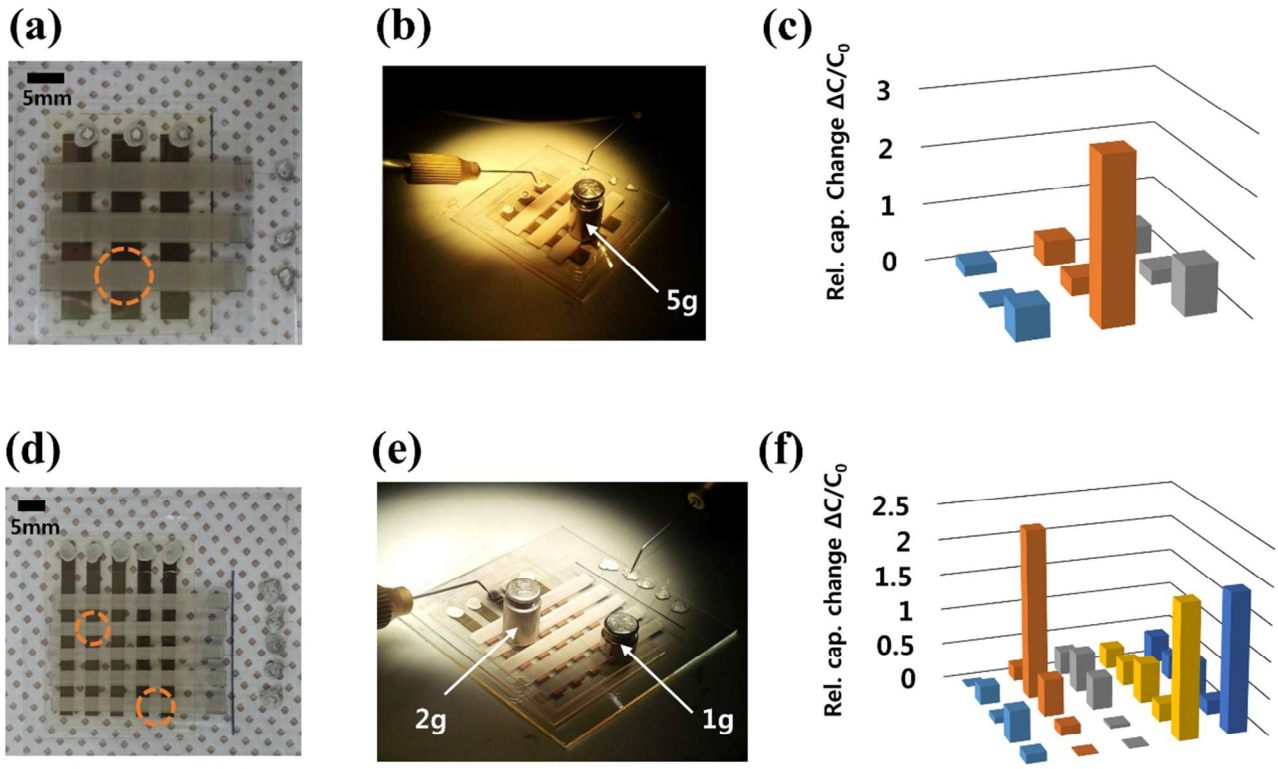

Fig. 5 Pixel-type pressure sensor arrays. (a) Photograph of the sensor array with 3 × 3 pixels. (b,c) 5g weight is loaded onto the 3 × 3 sensor array and the corresponding two-dimensional intensity profile is shown. (d) Photograph of the sensor array with 5 × 5 pixels. (e,f) 1g and 2g weights are loaded onto the 5 × 5 sensor array and the corresponding two-dimensional intensity profile is shown.

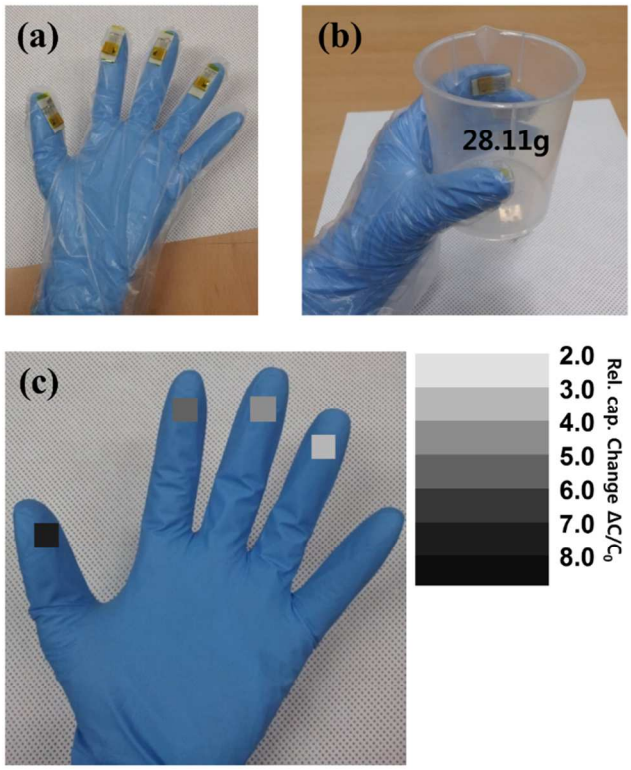

Fig. 6 Fingertip grip pressure sensing device. (a) Photograph of the fingertip grip pressure sensor. Each pressure sensor is attached on the fingertips. (b,c) Grabbing a plastic beaker with four fingertips and the corresponding relative capacitance changes are visualized.